SCIENTIFIC REP{O}RTS

OPEN

A decade of global volcanic SO$_2$ emissions measured from space

S. A. Carn[1], V. E. Fioletov[2], C. A. McLinden[2], C. Li[3,4] & N. A. Krotkov[4]

The global flux of sulfur dioxide (SO$_2$) emitted by passive volcanic degassing is a key parameter that constrains the fluxes of other volcanic gases (including carbon dioxide, CO$_2$) and toxic trace metals (e.g., mercury). It is also a required input for atmospheric chemistry and climate models, since it impacts the tropospheric burden of sulfate aerosol, a major climate-forcing species. Despite its significance, an inventory of passive volcanic degassing is very difficult to produce, due largely to the patchy spatial and temporal coverage of ground-based SO$_2$ measurements. We report here the first volcanic SO$_2$ emissions inventory derived from global, coincident satellite measurements, made by the Ozone Monitoring Instrument (OMI) on NASA's Aura satellite in 2005–2015. The OMI measurements permit estimation of SO$_2$ emissions from over 90 volcanoes, including new constraints on fluxes from Indonesia, Papua New Guinea, the Aleutian Islands, the Kuril Islands and Kamchatka. On average over the past decade, the volcanic SO$_2$ sources consistently detected from space have discharged a total of ~63 kt/day SO$_2$ during passive degassing, or ~23 ± 2 Tg/yr. We find that ~30% of the sources show significant decadal trends in SO$_2$ emissions, with positive trends observed at multiple volcanoes in some regions including Vanuatu, southern Japan, Peru and Chile.

Accurate inventories of the current spatial and temporal distribution of volcanic gas emissions to the atmosphere are required for numerous applications, ranging from baseline volcano monitoring to assessment of the impacts of volcanic degassing on the broader Earth system[1]. Sulfur species, principally sulfur dioxide (SO$_2$), are of most interest due to the ease of SO$_2$ measurement via ground- and satellite-based remote sensing[2,3] and their key role in the processes responsible for volcanic impacts on the environment, health, atmospheric chemistry and climate[4–7]. Recent advances in satellite remote sensing techniques have greatly improved constraints on the eruptive flux of SO$_2$ (and several other volatile species) from volcanoes[3,8–10], but the non-eruptive or passive volcanic degassing flux of SO$_2$ (hereafter, PVF) remains poorly constrained. In addition to its relevance for impact assessment, an accurate global volcanic SO$_2$ emissions inventory permits estimation of the volcanic output of other climate-relevant gas species and toxic trace metals (e.g., CO$_2$ and mercury[11,12]), and the identification of potential targets for ground-based gas sampling to measure the complete chemical and isotopic composition of volcanic gases. The most widely used existing volcanic SO$_2$ emissions inventory[13] is now several decades old, but its enduring popularity reflects the high demand for global volcanic SO$_2$ flux data.

Producing a database that faithfully reflects the contemporaneous PVF is a challenge due to the generally poor temporal and spatial coverage of ground-based volcanic gas measurements, which are often conducted on a campaign-style basis and/or during periods of heightened unrest[14–16] and are hence unlikely to accurately represent long-term average degassing rates. Although the geographic extent and frequency of ground-based volcanic SO$_2$ measurements is increasing[17], they remain sparse in many highly active volcanic regions such as Indonesia, Papua New Guinea, Vanuatu, the Aleutian Islands, the Kuril Islands and Kamchatka, and will be a formidable challenge in some very remote regions (e.g., the South Sandwich Islands, southern Atlantic Ocean). As a solution to this problem, we report here a new satellite-based volcanic SO$_2$ emissions inventory, based on more than a decade of measurements by the Ozone Monitoring Instrument (OMI) on NASA's Aura satellite[18], which is global in scope and provides estimates of the PVF from all of the strongest contemporary volcanic SO$_2$ sources. This new database, the first volcanic SO$_2$ emissions inventory to be derived from global, coincident measurements (rather than by collation of ground-based data widely distributed in space and time), benefits from several advantages of polar-orbiting satellite measurements, including global coverage and the use of a single, well-characterized sensor to detect and quantify all

[1]Department of Geological and Mining Engineering and Sciences, Michigan Technological University, Houghton, MI 49931, USA. [2]Air Quality Research Division, Environment and Climate Change Canada, Toronto, ON, Canada. [3]Earth System Science Interdisciplinary Center, University of Maryland, College Park, MD, USA. [4]Atmospheric Chemistry and Dynamics Laboratory, Code 614, NASA Goddard Space Flight Center, Greenbelt, MD 20771, USA. Correspondence and requests for materials should be addressed to S.A.C. (email: scarn@mtu.edu)
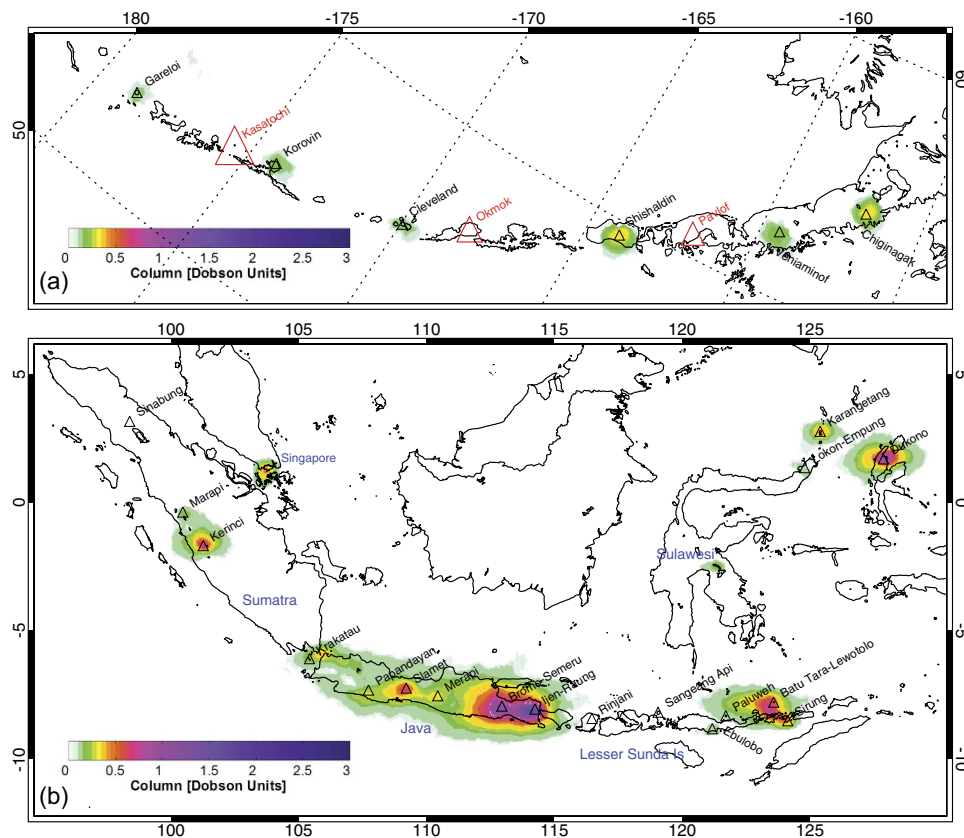
Figure 1. Mean SO$_2$ columns (in Dobson Units [DU]; 1 DU = 2.69 × 10^{16} molecules cm^{-2}) for 2005–2007 over (**a**) the Aleutian Islands (USA) and (**b**) Indonesia. The volcanic SO$_2$ sources (including paired sources) are labeled. The Aleutian map also shows locations of explosive eruptions since 2005 (*red triangles*), with symbol size proportional to total SO$_2$ emission[3,10]. The Indonesian map also shows anthropogenic SO$_2$ sources in Singapore and central Sulawesi, but does not show volcanic SO$_2$ emissions from Sinabung, Rinjani and Sangeang Api, which first appeared after 2007. Maps were generated using Interactive Data Language (IDL) version 8.5.1 (http://www.harrisgeospatial.com/).

SO$_2$ sources over the course of a long-term (multi-decadal) satellite mission. The use of a single instrument permits relatively straightforward reprocessing of archived data as SO$_2$ retrieval algorithms improve, offering increasing sensitivity to volcanic SO$_2$[19]. Furthermore, unlike many spectroscopic instruments used for ground-based SO$_2$ measurements, satellite instruments such as OMI are also subject to intensive calibration and validation[20].

Although satellites have been used to measure eruptive SO$_2$ emissions for several decades[3,8,21,22], their use for quantification of passive volcanic degassing is relatively recent and concurrent with the advent of sufficiently sensitive space-borne instruments, such as OMI[23–25]. Previous application of OMI SO$_2$ data to detection of non-eruptive volcanic degassing has focused on the stronger SO$_2$ sources, detectable from space on a near-daily basis[3,16,25]. As recently demonstrated[26–30], with specialized data processing techniques it is possible to enhance the sensitivity of ultraviolet (UV) satellite SO$_2$ measurements to enable detection of persistent anthropogenic SO$_2$ sources emitting on the order of 30 kilotons/year (kt/yr; equivalent to ~80 tons/day [t/d]), with the detection limit expected to be even lower for SO$_2$ sources located at high elevation (including many volcanoes). Here, we present a new global volcanic SO$_2$ emissions inventory derived from application of these techniques to more than a decade of OMI observations (2005–2015), which represents a timely replacement for existing databases[13,31]. We also compare the satellite-based SO$_2$ fluxes to a recent compilation of independent ground-based measurements[31], and other sources, and examine the global distribution of volcanic SO$_2$ fluxes to reveal regional- and arc-scale trends in volcanic degassing.

Data and Methods

Volcanic SO$_2$ emissions were estimated using a new operational OMI planetary boundary layer (PBL) SO$_2$ column dataset produced using a principal component analysis (PCA) algorithm[32]. A detailed description of the techniques used to identify SO$_2$ sources (both anthropogenic and volcanic) and calculate emissions is given in ref. 29, and is briefly summarized here. The OMI PCA SO$_2$ data used in the analysis were restricted to 'clear sky' conditions by including only those OMI pixels with a cloud radiance fraction below 20%; solar zenith angles were also restricted to <70° to reduce noise at high latitudes. In addition, all pixels affected by the OMI row anomaly data gap since 2007 (see: http://www.knmi.nl/omi/research/product/rowanomaly-background.php) were excluded. After pixel screening, an OMI pixel averaging or oversampling procedure[26,27] is used to resolve potential locations of SO$_2$ emissions and produce global maps similar to those shown in Fig. 1. To further enhance
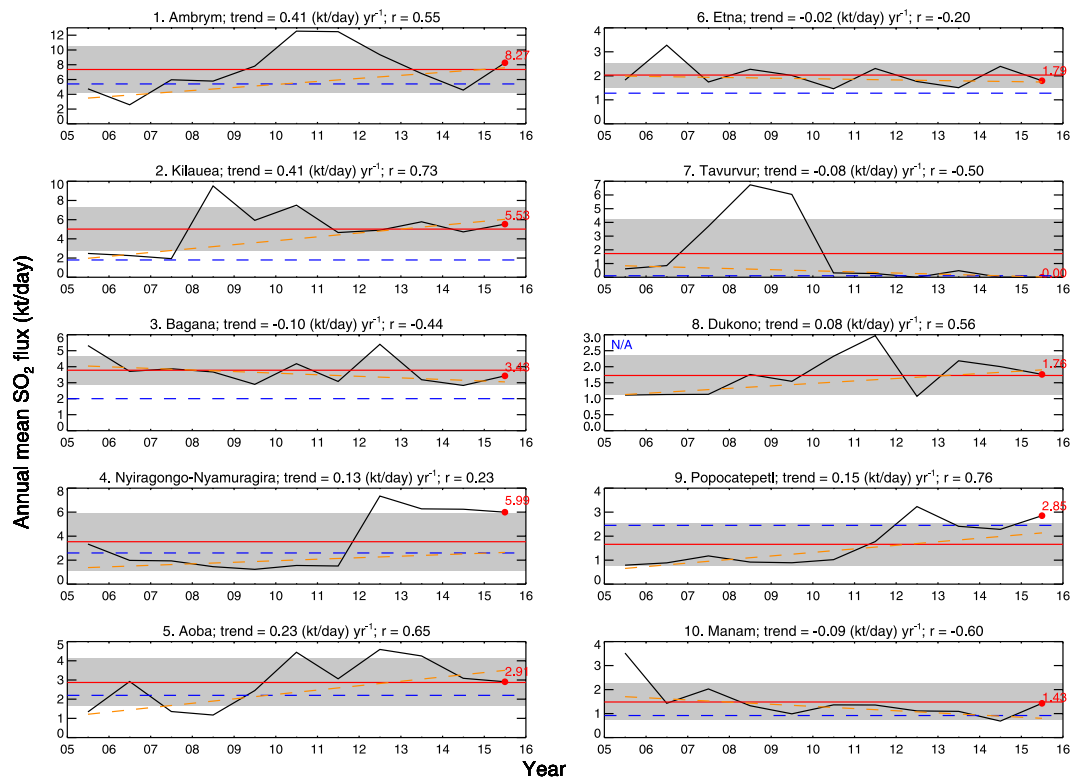
Figure 2. OMI-derived annual mean SO$_2$ fluxes in 2005–2015 for the ten strongest volcanic SO$_2$ sources (including paired sources) in the inventory. Plots are titled with the volcanic source name and rank, and the trend (slope) and linear correlation coefficient (*r*) of an error-weighted linear regression fit of the annual mean SO$_2$ fluxes. Each plot shows the annual mean SO$_2$ fluxes (*solid black line*), mean SO$_2$ flux in 2015 (*labeled red dot*), linear regression trend line (*dashed orange line*), decadal mean SO$_2$ flux (*horizontal red line*), ±1 standard deviation of the decadal mean SO$_2$ flux (*gray band*), and an independent estimate of SO$_2$ flux (*horizontal dashed blue line*) from a recent compilation[13] or another source. Here, SO$_2$ flux data for Etna and Popocatepetl are from refs 58 and 59, respectively. If no independent measurements are available, the plot is labeled with 'N/A'. See Supplementary Figures (Figs S9–S16) for similar plots for all other sources.

the SO$_2$ signal and identify sources, a wind rotation technique is applied to align all the OMI SO$_2$ observations for each source along the same wind vector[30], and then SO$_2$ emissions are estimated by fitting an exponentially modified Gaussian function to the OMI data[33]. The variable altitude of passive volcanic SO$_2$ plumes is accounted for by applying an air mass factor (AMF) correction to the OMI PBL SO$_2$ columns based on volcano altitude. To calculate accurate estimates of the SO$_2$ PVF, the effects of volcanic eruptions generating transient, large SO$_2$ column amounts are removed by applying a threshold SO$_2$ column amount of 5–15 Dobson Units (DU) to the OMI SO$_2$ data. This threshold was selected based on typical SO$_2$ column amounts measured by OMI in passive and eruptive volcanic plumes. However, we note that at some volcanoes it may be impossible to completely separate passive (i.e., involving no coincident eruption of magma) from eruptive SO$_2$ emissions, or even to establish which mode of degassing dominates at any given time. This is particularly problematic at volcanoes undergoing lava dome extrusion (e.g., Merapi, Indonesia; Soufriere Hills, Montserrat) or persistent Vulcanian or Strombolian activity (e.g., Stromboli, Italy; Fuego, Guatemala; Sakura-jima, Japan; Yasur, Vanuatu). Hence, while we believe that passive SO$_2$ degassing is the dominant process responsible for the emissions reported here, a contribution from eruptive degassing is inevitable at some volcanoes, as is the case for previous SO$_2$ emissions inventories[13,31]. Total uncertainties (including contributions from AMF, SO$_2$ mass, SO$_2$ lifetime, and wind speed uncertainty) on annual SO$_2$ flux estimates are 55% and >67% for sources emitting more than 100 kt/yr and under 50 kt/yr, respectively[29]. Some of the largest individual sources of error are systematic and hence will introduce a bias in absolute SO$_2$ flux values but will not affect relative inter-annual flux variability (Fig. 2).

For the inventory presented here, volcanic SO$_2$ sources were identified based on 3-year averages of OMI data for 2005–2007, 2008–2010 and 2011–2014, then annual emissions were calculated for each source for the entire 11-year period studied (2005–2015). Note that the aforementioned 30 kt/yr (~80 t/d) detection limit was determined based on OMI observations of power plant SO$_2$ emissions in the eastern USA[28], which are typically confined to the PBL. The higher altitude of volcanic SO$_2$ plumes translates into a higher AMF (greater sensitivity), which reduces the detection limit to values as low as ~6 kt/yr (~16 t/d). The detection limit will be lowest for low-latitude volcanoes, which benefit from more satellite observations under optimal conditions (e.g., low solar zenith angles). To assess the presence of significant decadal trends in the SO$_2$ emissions, we applied a weighted linear regression fit to the annual SO$_2$ emissions for each source, using the 1σ emission uncertainties (Supplementary Table S1) to weight the data, to derive a trend and linear correlation coefficient (*r*). Although it

Rank[1]	Volcano[2]	Country	Mean SO$_2$ flux (t/d)	1σ (t/d)	Prev. SO$_2$ flux (t/d)[3]
1	Ambrym (1)	Vanuatu	7356	3168	5400
2	Kilauea (3)	USA	5019	2275	1800
3	Bagana (4)	Papua New Guinea	3779	886	2000
4	Nyiragongo + Nyamuragira (2)	Democratic Republic of Congo	3533	2408	2600
5	Aoba (6)	Vanuatu	2870	1229	2200
6	Mt. Etna (9)	Italy	2039	522	1277
7	Tavurvur (82)	Papua New Guinea	1729	2535	110
8	Dukono (10)	Indonesia	1726	611	—
9	Popocatepetl (7)	Mexico	1658	893	2450
10	Manam (12)	Papua New Guinea	1484	753	180
11	Yasur (8)	Vanuatu	1408	563	633
12	Anatahan (83)	Northern Mariana Islands	1335	1867	4367
13	Soufriere Hills (42)	Montserrat (UK)	1296	761	574
14	Nevado del Ruiz (5)	Colombia	1074	1376	1900
15	Sakura-jima (35)	Japan	1056	757	1640
16	Miyake-jima (63)	Japan	1018	934	2120
17	Karymsky (14)	Russia	911	250	75
18	Masaya (18)	Nicaragua	867	364	800
19	Suwanose-jima (17)	Japan	863	314	670
20	Bromo + Semeru (13)	Indonesia	775	298	212
21	Mutnovsky + Gorely (55)	Russia	753	690	1030
22	Turrialba + Poas (16)	Costa Rica	751	681	2754
23	Kizimen (84)	Russia	711	1544	100
24	Avachinsky (26)	Russia	707	619	—
25	Lewotolo + Batu Tara (28)	Indonesia	632	177	—
26	Ijen + Raung (19)	Indonesia	631	238	—
27	Ulawun (24)	Papua New Guinea	630	581	640
28	Langila (48)	Papua New Guinea	629	527	250
29	Aso (11)	Japan	628	492	410
30	Nevado del Huila (44)	Colombia	627	665	—
31	San Cristobal + Telica (25)	Nicaragua	621	283	690
32	Satsuma-Iwojima (20)	Japan	585	190	574
33	Pagan (73)	Northern Mariana Islands	583	547	—
34	Kliuchevskoi + Bezymianny (32)	Russia	580	461	700
35	Shiveluch (31)	Russia	530	284	500
36	Chikurachki + Ebeko (21)	Russia	496	468	100
37	Mayon (60)	Philippines	453	274	530
38	Asama (15)	Japan	449	430	360
39	Gaua (30)	Vanuatu	434	382	2959
40	Sirung (29)	Indonesia	373	162	—
41	Redoubt (85)	USA	368	1051	657
42	Shishaldin (23)	USA	347	278	—
43	Tungurahua (46)	Ecuador	342	235	1460
44	Copahue (22)	Chile	341	425	—
45	Sinabung (36)	Indonesia	327	595	—
46	Karangetang (33)	Indonesia	313	85	—
47	Krakatau (58)	Indonesia	303	252	190
48	Kerinci (45)	Indonesia	294	99	—
49	Tofua (56)	Tonga	284	89	—
50	Villarrica (41)	Chile	281	160	320
51	Michael (43)	South Sandwich Isl. (UK)	263	63	—
52	Sarychev (54)	Russia	260	324	100
53	Tinakula (86)	Solomon Islands	256	276	—
54	Veniaminof (87)	USA	255	214	—
55	White Island (49)	New Zealand	254	107	430
56	Fuego + Pacaya (50)	Guatemala	252	46	280

Continued

Rank[1]	Volcano[2]	Country	Mean SO$_2$ flux (t/d)	1σ (t/d)	Prev. SO$_2$ flux (t/d)[3]
57	Lastarria (39)	Chile	248	62	884
58	Santa Maria (52)	Guatemala	247	119	120
59	Barren Island (72)	India	243	341	—
60	Ubinas (37)	Peru	222	252	—
61	Galeras (88)	Colombia	218	317	450
62	Bulusan (70)	Philippines	206	199	370
63	Slamet (38)	Indonesia	206	132	58
64	Reventador (57)	Ecuador	206	187	450
65	Lokon-Empung (59)	Indonesia	204	154	—
66	Korovin (65)	USA	198	160	—
67	Kudriavy (74)	Russia	187	103	90
68	Stromboli (53)	Italy	181	82	200
69	Cleveland (77)	USA	152	142	—
70	Montagu (62)	South Sandwich Isl. (UK)	142	179	—
71	Ketoi (79)	Russia	139	151	—
72	Chiginagak (69)	USA	138	127	—
73	Tokachi (61)	Japan	135	98	175
74	Piton de la Fournaise (34)	Reunion Island, France	134	162	—
75	Spurr (64)	USA	106	106	106
76	Jebel at Tair (89)	Yemen	103	295	—
77	Santa Ana (78)	El Salvador	97	180	120
78	San Miguel (51)	El Salvador	88	134	260
79	Sabancaya (27)	Peru	87	158	—
80	Ebulobo (67)	Indonesia	86	63	—
81	Isluga (68)	Chile	78	107	—
82	Rinjani (40)	Indonesia	74	131	—
83	Augustine (75)	USA	73	140	48
84	Sangeang Api (47)	Indonesia	71	150	—
85	Kanlaon (81)	Philippines	70	182	—
86	Alu-Dalafilla + Erta Ale (71)	Ethiopia	64	24	60
87	Paluweh (76)	Indonesia	60	65	—
88	Gareloi (66)	USA	52	47	—
89	Erebus (80)	Antarctica	52	31	74
90	Marapi (90)	Indonesia	34	34	—
91	Merapi (91)	Indonesia	32	51	140
	TOTAL:		**62965**		

Table 1. Mean SO$_2$ fluxes (2005–2015) for sources of passive volcanic SO$_2$ degassing detected by OMI.
[1]Rank based on mean SO$_2$ flux for 2005–2015. [2]Number in parentheses indicates SO$_2$ flux rank in 2015, the most recent year analyzed. [3]Previously reported SO$_2$ flux, if available. All fluxes are derived from [13] or [31], except data for Etna[58], Popocatepetl[59], Anatahan[15], Bromo-Semeru[41,44], Turrialba[24], Gaua[36], Redoubt[60], Krakatau[42], Lastarria[55] and Spurr[61].

is possible to use satellite data to estimate SO$_2$ fluxes on much shorter timescales for strong sources[9,25], the focus here is on long-term average emissions and trends rather than short-term variations. Future updates to the volcanic SO$_2$ emissions inventory will benefit from the recent release of new OMI PCA SO$_2$ products tailored to the variable injection height of volcanic plumes[19], which should further reduce the uncertainties.

Results and Discussion

A total of 91 persistently degassing volcanic SO$_2$ sources have been detected in OMI measurements between 2005 and 2015 (Table 1; Supplementary Fig. S1). However, some of the detected SO$_2$ signals originate from paired sources (see below), so the actual number of volcanoes contributing to the detected SO$_2$ emissions is probably at least 100. For comparison, the Andres and Kasgnoc (1998) inventory[13] includes 49 continuously emitting sources. Since 3-year averages of OMI SO$_2$ data were used to identify the sources, the main criterion for detection is persistent emissions on that timescale. Hence it is possible that volcanoes exhibiting shorter-duration episodes of passive degassing may elude detection, but may subsequently be identified in more detailed analysis of shorter time periods. Table 1 lists the volcanic SO$_2$ sources, ranked according to their mean SO$_2$ flux for the entire 11-year period analyzed. Maps of the volcanic SO$_2$ sources are shown in Fig. 1 and Supplementary Figs S1–S8. Figure 2 and Supplementary Figures (Supplementary Figs S9–S16) show the variation in annual mean SO$_2$ fluxes at each
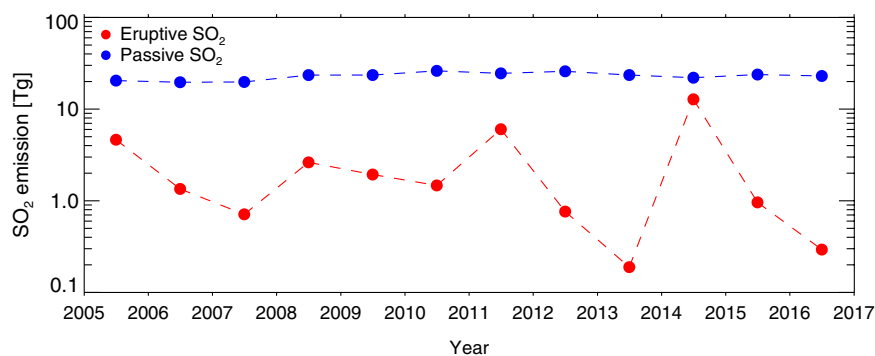
Figure 3. Total, global eruptive and passive volcanic SO$_2$ emissions (in Tg; 1 Tg = 10^{12} g) in 2004–2016. Eruptive emissions are derived from [10] and recent updates; passive emissions are from the inventory described here. Passive volcanic SO$_2$ emissions in 2016 are assumed to continue at the mean annual rate observed in 2005–2015.

source, with correlative ground-based SO$_2$ measurements if available, and the trends and linear correlation coefficients (*r*) derived from a weighted linear regression of the annual emissions. The complete dataset, including annual emissions for each volcano, is provided in a Supplementary Table (Supplementary Table S1).

One of the disadvantages of UV satellite measurements is low spatial resolution, and as a result SO$_2$ emissions from clustered degassing volcanoes (within ~50 km) cannot be distinguished. Hence, some SO$_2$ emissions in the inventory are attributed to paired sources (e.g., Fig. 2), such as Nyiragongo-Nyamuragira (DR Congo), Bromo-Semeru (East Java, Indonesia) and Batu Tara – Lewotolo (Lesser Sunda Islands, Indonesia). Kamchatka (Russia) is another region where assignment of SO$_2$ emissions to specific volcanoes can be problematic (e.g., Mutnovsky – Gorely). Emissions reported for Chikurachki in the northern Kuril Islands may include a contribution from Ebeko (Table 1), where SO$_2$ emissions of ~100 t/d have been reported[34]. Resolving these merged SO$_2$ sources will require further field-based measurements in some regions, or the use of satellite data with higher spatial resolution[35].

Notwithstanding some drawbacks, the strength of a satellite-derived emissions inventory is the global coverage. Most of the dominant sources (e.g., Ambrym, Kilauea, Bagana, Etna) are well established from prior measurements[14,16,36,37]. However, the OMI measurements (Table 1; Fig. 2) reveal, in some cases for the first time, significant, persistent SO$_2$ degassing at remote volcanoes in the South Sandwich Islands (Michael and Montagu), the Kuriles (Ketoi, Kudriavy), the Aleutians (Gareloi, Korovin), Indonesia (e.g., Dukono, Batu Tara - Lewotolo, Sirung, Ebulobo), and the southwest Pacific (e.g., Tofua, Tinakula). Gas emissions from Erebus (Antarctica) are also detected from space for the first time (Table 1; Supplementary Fig. S16). The OMI database thus provides what is the first truly global picture of contemporary volcanic SO$_2$ degassing, including sources where acquisition of frequent ground-based data will remain highly challenging.

Weighted linear regression reveals a range of temporal trends in the SO$_2$ fluxes (Fig. 2; Supplementary Figs S9–S16). We acknowledge that a simple linear trend may not be applicable to many of the volcanic SO$_2$ sources (indicated by a low correlation coefficient, $-0.5 \leq r \leq 0.5$; Fig. 2; Supplementary Figs S9–S16), but a detailed exploration of the trends in SO$_2$ emissions at each volcano is beyond the scope of this study. Nevertheless, the SO$_2$ data for some sources clearly indicate a long-term decline in SO$_2$ discharge (e.g., Miyakejima, Manam, Soufriere Hills; Fig. 2, Supplementary Fig. S9). A weak or insignificant trend in SO$_2$ emissions likely reflects relatively stable emissions (e.g., Bagana, Etna; Fig. 2), or more pulsatory degassing (e.g., Tavurvur, Anatahan, Huila; Fig. 2, Supplementary Figs S9 and S10); the latter could reflect cycles of magma intrusion followed by protracted gas release. Three of the top four sources feature active basaltic lava lakes (Ambrym, Kilauea and Nyiragongo-Nyamuragira), and in these cases the peak SO$_2$ discharge can be clearly linked to the establishment of new and/or larger lava lakes (e.g., at Kilauea in 2008[38] and Nyamuragira in 2012[35]). The significance of the observed trends in SO$_2$ emissions is discussed further below.

In summing the SO$_2$ emissions from all detected sources, we find that the total annual SO$_2$ PVF is remarkably stable at 23.0 ± 2.3 Tg/yr (the highest annual total in the past decade was ~26 Tg in 2010). Andres and Kasgnoc (1998)[13] estimated a total non-eruptive volcanic SO$_2$ flux of ~12 Tg/yr for the 1970–1997 period (including a power-law extrapolation to estimate the contribution from unmeasured volcanoes); our higher estimate reflects the inclusion of more strong sources emitting >1000 t/d SO$_2$ (Table 1). A comparison with eruptive SO$_2$ fluxes[3,10] confirms the common assumption that the SO$_2$ PVF is typically around an order of magnitude larger (Fig. 3), except during years with major SO$_2$-rich eruptions such as at Bárðarbunga-Holuhraun (Iceland) in 2014[39]. The average total SO$_2$ PVF from all detectable sources is ~63 kt/day (2005–2015 mean; Table 1), which is broadly commensurate with a global SO$_2$ PVF of ~50.6 kt/day estimated by ref. 31 using a sparser dataset. Fluxes of SO$_2$ during large eruptions (e.g., Holuhraun[39]) can greatly exceed the total PVF on short timescales.

The new volcanic SO$_2$ emissions inventory includes numerous previously unquantified sources. Based on SO$_2$ data reported in the literature (and we acknowledge that a substantial amount of SO$_2$ emissions data collected by volcano observatories may not be published), we find that 36 of the 91 sources (i.e., ~40%) have no previously reported SO$_2$ flux. The most prominent of these is Dukono (Halmahera, Indonesia), ranked 8th in our inventory (Table 1; Figs 1 and 2), but many of the stronger sources have relatively few SO$_2$ flux determinations. Based on

recent compilations[31], 38 volcanoes (i.e., ~68% of the 56 volcanoes with prior measurements) have reported SO_2 fluxes within the 1σ fitting uncertainty of the OMI-derived fluxes. For ~41% of the sources with prior measurements, the OMI-derived SO_2 flux exceeds the independent estimate by at least 20%, and for ~36% the reverse is true (Fig. 2; Supplementary Figs S9–S16), whilst for the remainder (e.g., Ulawun, San Cristobal, Satsuma-Iwojima, Masaya, Fuego; Supplementary Figs S9–S16) the satellite- and ground-based SO_2 emission rates show excellent agreement (to within 20%). Nonetheless, it is notable that the OMI-derived SO_2 fluxes for most of the strongest sources are higher than previous estimates (Table 1; Fig. 2). For several sources (e.g., Ambrym, Bagana, Aoba, Manam) we believe that this is real and a result of infrequent prior measurements at these very active volcanoes coupled with significant variability in SO_2 emissions. Furthermore, at Kilauea, where a significant discrepancy is observed (Fig. 2), it has recently been shown[37] that ground-based techniques can underestimate SO_2 emissions by a factor of 2 or more in dense plumes. However, with the exception of the high-flux volcanoes, we observe no significant high or low bias in the OMI-derived SO_2 fluxes, but more detailed validation of the derived SO_2 emissions is certainly required.

In addition to Dukono, the new database sheds considerable light on the SO_2 flux from other Indonesian volcanoes (Fig. 1), which is noteworthy given the generally poor constraints on volcanic emissions in the archipelago[40,41]. Dukono (Halmahera) is the strongest volcanic SO_2 source with no prior constraints on its SO_2 flux (Figs 1 and 2). The SO_2 signal in the Sunda Strait near Krakatau volcano (Fig. 1) was previously assigned to the Suralaya power plant in Cilegon, West Java[29], but we now assume this to be dominated by volcanic emissions from Krakatau (Table 1). SO_2 emissions of 190 ± 40 t/d were reported at Krakatau in 2014[42], well above the satellite detection limit, so if this is a sustained SO_2 flux then it seems likely that most of the detected SO_2 is volcanic. The OMI-derived SO_2 flux for Krakatau is 303 ± 252 t/d (Table 1), i.e., within the range of ground-based measurements[42]. Degassing from Papandayan (West Java[40]) may also be detected in the OMI data (Fig. 1), although it is difficult to isolate from the larger SO_2 signal associated with Slamet and hence is not treated as a separate source here. As noted earlier, several Indonesian volcanoes in East Java and the Lesser Sunda Islands are difficult to resolve using the OMI measurements, thus the reported emissions for Bromo and Semeru, Raung and Ijen, and Batu Tara and Lewotolo represent aggregated fluxes (Table 1). Ground-based SO_2 measurements in Indonesia are also increasing in frequency and coverage[40–44]. The OMI-derived average SO_2 flux from Bromo-Semeru (775 ± 298 t/d; Table 1) is higher than combined ground-based estimates for these volcanoes (~200 t/d[41,44]), but the ground-based campaigns only cover a few days of degassing. It is also possible that the satellite measurements are more effective than ground-based techniques at constraining SO_2 flux at volcanoes that exhibit transitions from purely passive degassing to degassing via Vulcanian explosions (e.g., Semeru), due to the difficulty of measuring SO_2 in proximal ash-laden plumes[44].

Another notable feature apparent in the map of Indonesian SO_2 sources is that some regions show lower emissions or an absence of subaerial SO_2 degassing, despite the presence of numerous Holocene volcanoes; e.g., southern Sumatra and the western Lesser Sunda Islands (Fig. 1). It is perhaps no coincidence that the latter region is the location of several volcanoes responsible for large SO_2-rich explosive eruptions (linked to significant climate impacts[5]) including Agung (1963)[45], Samalas (1257)[46] and Tambora (1815)[47]. The identification of such degassing gaps, where stored gas may be accumulating in magma reservoirs rather than being released to the atmosphere, could assist hazard mitigation and identification of potential sites of future explosive eruptions. The mutually exclusive relationship between strong subaerial SO_2 degassing and large explosive eruptions during the past decade is also apparent in the Aleutian Islands (Fig. 1).

Further corroboration of the OMI-derived SO_2 emissions is possible based on data collected at Japanese volcanoes. A recent assessment[48] showed that 94% of the total volcanic SO_2 flux in Japan originates from 6 volcanoes: Tokachi, Asama, Aso, Sakurajima, Satsuma-Iwojima, and Suwanosejima; plus Mijake-jima after 2000. A total of 17 degassing volcanoes are documented in Japan[48]. OMI is able to detect all seven of the strongest sources (Table 1), yielding a time-averaged total SO_2 flux for Japan of 1.73 Tg/yr in 2005–2015, which is commensurate with a total SO_2 flux of 2.2 Tg/yr (including the intense degassing from Miyake-jima after 2000, which continues to subside) or 1.4 Tg/yr pre-2000 based on ground-based data[48]. Thus the OMI measurements represent an accurate estimate of total volcanic SO_2 emissions from Japan during the ongoing waning phase of Miyake-jima's degassing activity.

Examination of the frequency-flux relationship of volcanic SO_2 fluxes in Japan reveals that they do not fit a power law distribution[48], as had been previously suggested for the global flux distribution[49]. A frequency-flux plot for the OMI-derived SO_2 emissions confirms that the global volcanic SO_2 sources also do not follow a power law distribution (Fig. 4). We also find a clear 'roll-off' of the distribution at an SO_2 flux of ~500–600 t/d, remarkably similar to that found in the ground-based Japanese SO_2 flux data[48]. This important result shows that the distribution of volcanic SO_2 emissions on the scale of individual arcs can indeed mimic the global distribution, provided that large flux datasets are available from a range of source strengths (i.e., including very strong emitters such as Miyake-jima). It also indicates that the global volcanic SO_2 flux is dominated by the ~30 largest sources (Table 1; Fig. 4), and quantifying the flux from these volcanoes would provide a good estimate of the global SO_2 flux (in our database the 30 strongest sources emit ~80% of the total flux).

Arc-scale trends in volcanic degassing.
Another significant application of the global satellite SO_2 measurements is the potential for detection of arc-scale trends in gas flux. Global, consistent SO_2 measurements such as the OMI-derived database presented here pave the way to new insights into arc-scale volcanic processes, including correlations between volcanic SO_2 emissions and other geophysical parameters such as arc length and subduction rate, since they provide a synoptic perspective on degassing that is not easily obtained from other techniques. The application of pattern recognition techniques to global SO_2 emissions data, such as the example in Fig. 5 (also see Supplementary Fig. S17), will permit an epidemiological approach whereby analogous
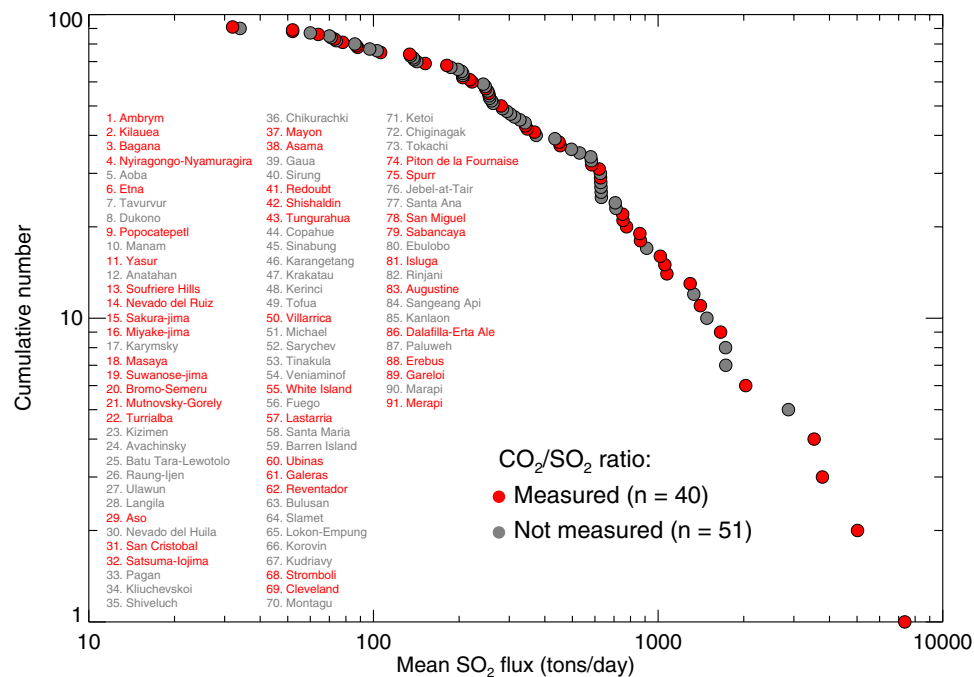
Figure 4. Cumulative frequency – SO$_2$ flux plot for all volcanic SO$_2$ sources detected by OMI. Symbol color indicates whether the CO$_2$/SO$_2$ ratio of the volcanic gases has been measured as of October 2016. Information on availability of CO$_2$/SO$_2$ ratios is from E. Hauri (DCO-DECADE, pers. comm.).

degassing patterns may be identified at similar volcanic systems on regional or global scales. Interpretation of SO$_2$ data at individual volcanic systems can be ambiguous[50], but analysis of arc-scale SO$_2$ measurements potentially allows the identification of correlated trends at multiple volcanoes that can be more confidently ascribed to similar volcanic processes.

The recent status of SO$_2$ emissions at the detected volcanic sources can be straightforwardly assessed by comparing the most recently measured annual mean SO$_2$ flux (for 2015) with the decadal mean flux (Supplementary Figs S1 and S17). This simple metric shows some notable arc-scale consistency in several regions; for example, all the detected volcanic SO$_2$ sources in Peru and Chile (Isluga, Villarrica, Lastarria, Ubinas, Copahue, and Sabancaya) have measured emissions in 2015 that are above the long-term average (Supplementary Figs S1 and S17). In southern Peru, both Ubinas and Sabancaya show particularly anomalous SO$_2$ emissions in 2015 (Table 1; Supplementary Figs S1 and S17), suggesting that these volcanoes are currently in a period of elevated activity. In contrast, the volcanoes of Papua New Guinea (Tavurvur, Langila, Bagana, Manam, and Ulawun) all show recent SO$_2$ emissions close to or below the decadal mean (Supplementary Figs S1 and S17).

A more rigorous evaluation of trends in SO$_2$ emissions must be restricted to those sources with annual SO$_2$ emissions showing a significant positive or negative linear correlation coefficient (i.e., $r \leq -0.5$ or $r \geq 0.5$; Fig. 5). Using this criterion, 32 volcanoes show significant decadal trends in SO$_2$ emissions (Fig. 5), and although we highlight some potential arc-scale correlations here, further detailed analyses and other measurements are required to evaluate these findings. Trend analysis reveals that most volcanoes in the Vanuatu arc (Ambrym, Aoba and Yasur) show increased degassing in 2005–2015 (Fig. 5), and the only other detectable volcanic SO$_2$ source in Vanuatu (Gaua) also shows a positive trend but with a weaker correlation coefficient ($r = 0.38$; Supplementary Fig. S11). Both Ebulobo and Paluweh (Flores, Indonesia) show significant positive trends (Fig. 5) and are located in the same region of the Sunda arc (Fig. 1). In the Ryukyu Islands and Kyushu regions of Japan, SO$_2$ emissions from Satsuma-Iwojima, Sakura-jima, and Aso all show significant positive trends in 2005–2015 (Fig. 5), and the only other detected volcanic SO$_2$ source in this region (Suwanose-jima) also shows a positive trend with a lower correlation coefficient ($r = 0.39$; Supplementary Fig. S9). In addition, there is independent evidence for increased volcanic activity in the Ryukyu Islands and Kyushu region, including a significant eruption at Aso in October 2016, and elevated unrest at Sakura-jima[51]. A recent study[51] presents geophysical evidence for magma accumulation at Sakura-jima in the 1996–2007 period, with potential for a repeat of its 1914 Plinian eruption in ~25–30 years. The OMI SO$_2$ observations show a substantial increase in SO$_2$ degassing from Sakura-jima, particularly in 2011–13 (Fig. 5), indicating that the volcano was releasing more gas in this period largely via an increased frequency of vulcanian eruptions[51]. However, since 2013 the SO$_2$ emissions from Sakura-jima have declined below the decadal mean (Fig. 5), and so the future evolution of its activity is unclear. Nevertheless, the observed degassing over the past decade may have important implications for future activity at Sakura-jima. For example, the sustained release of SO$_2$ could be 'defusing' the potential climate impact of a future Plinian eruption, and/or could render a combined explosive-effusive eruption (such as the 1914 event) more likely due to limited gas supply. Gas overpressure and compressibility are rarely factored into models of volcano deformation[52] and the SO$_2$ emissions could also indicate a contribution to the deformation signal due to volatile overpressure in the magma reservoir.
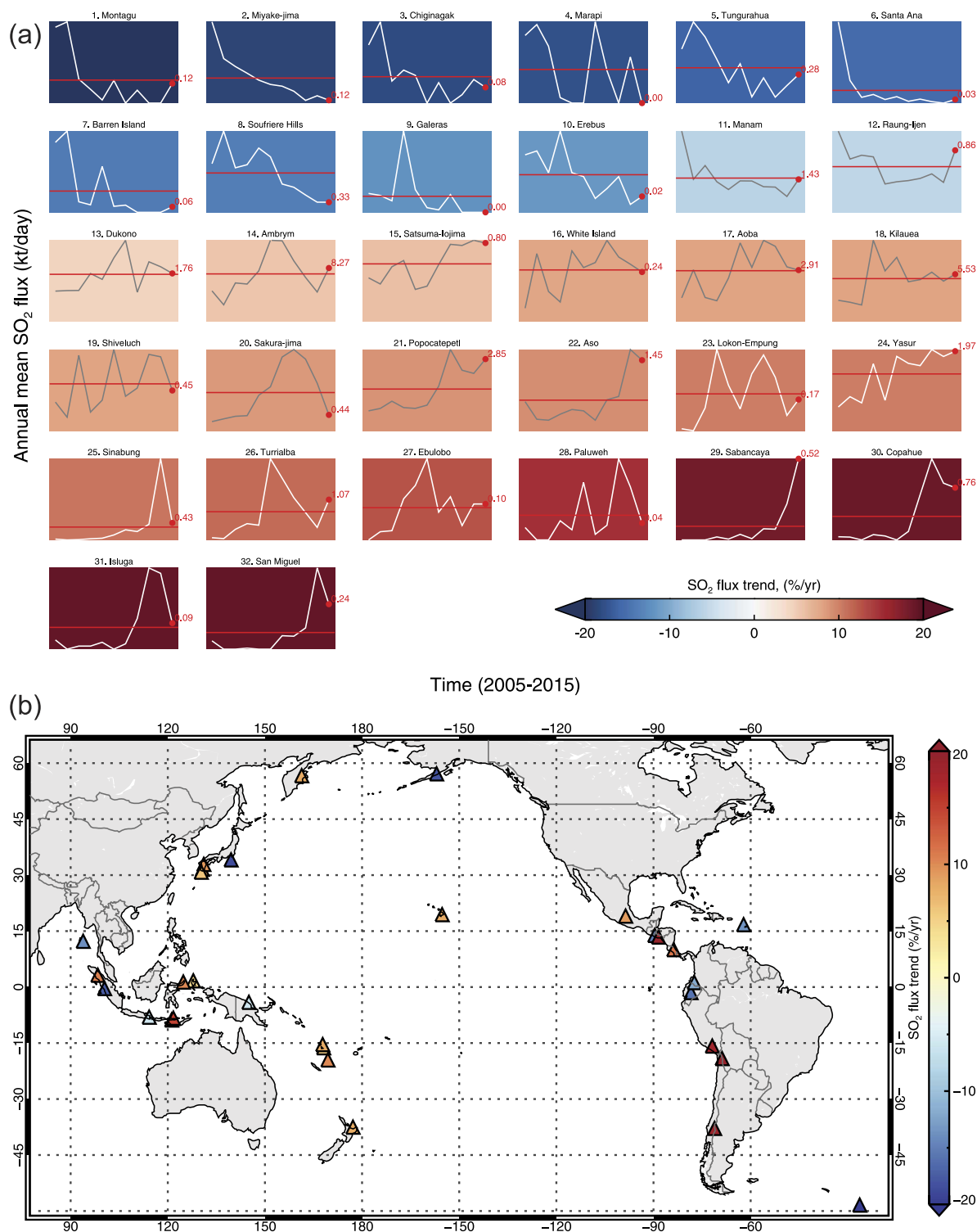
Figure 5. (**a**) Decadal trends in SO_2 emissions measured at 32 volcanic SO_2 sources showing a significant linear correlation coefficient from a weighted linear regression fit ($r \leq -0.5$ or $r \leq 0.5$). Plots are ranked in order of calculated SO_2 flux trend (i.e., the slope of the linear fit) from negative to positive values. Hence, cold and warm colors indicate sources showing a significant reduction or increase in SO_2 emissions over the 11-year period of measurements, respectively. Each individual plot shows the annual mean SO_2 fluxes for 2005–2015 (*white-gray line*), the decadal mean SO_2 flux (*red line*) and the annual mean SO_2 flux in 2015 (*labeled red dot*) for each source; axis labels are omitted for clarity. The vertical scale on each plot extends from zero to the maximum measured SO_2 flux. For more detailed time-series plots, see Fig. 2 and Supplementary Figures (Figs S9–S16); (**b**) Location map of the 32 volcanic SO_2 sources, colored based on SO_2 flux trend in 2005–2015 (also see Supplementary Figure S1). Map generated using Interactive Data Language (IDL) version 8.5.1 (http://www.harrisgeospatial.com/).

In summary, while the correlated trends in SO_2 emissions observed in some arcs could be purely coincidental, possible links to underlying regional- or arc-scale geophysical processes (e.g., a coincident pulse in shallow magma supply) merit further investigation but cannot be confirmed on the basis of SO_2 emissions alone. Regardless of the underlying cause, our trend analysis (Fig. 5) provides new insight into the locations of increased volcanic SO_2 degassing over the past decade, which would be good targets for increased monitoring (if not already in place), and into volcanoes undergoing long-term decline.

Pre-eruptive volcanic degassing.　Global satellite-based SO_2 surveillance also offers the potential for detection of pre-eruptive degassing at reawakening volcanoes. As noted above, increased SO_2 emissions at Aso (Japan) beginning in 2011 (Fig. 5; Supplementary Fig. S10) preceded eruptions in 2014–2016[53]. SO_2 emissions were detected at Sarychev Peak (Kuril Islands) in 2005–2008 and showed a modest increase prior to its large eruption in June 2009[3] (Supplementary Fig. S13). At Alu-Dalafilla (Ethiopia), weak but detectable SO_2 emissions were present in 2005–2007 (Supplementary Fig. S16) prior to an unexpected eruption in November 2008[3]. A shallow (~1 km deep) magma chamber has been identified at Alu-Dalafilla[54], refilling after the 2008 eruption, which is a likely source of the pre-eruptive SO_2 emissions. Ground deformation data and the longevity of the magmatic system are consistent with the existence of a relatively thick sill[54]; the persistent low SO_2 flux detected from 2005–2014 (Supplementary Fig. S16) also supports this, although it is possible that some of the SO_2 detected by OMI may originate from nearby Erta 'Ale volcano. Continued analysis of global space-based SO_2 measurements will thus be valuable for volcanic hazard assessment, particularly at unmonitored volcanoes. Although the low temporal resolution of annual mean SO_2 emissions precludes timely identification of pre-eruptive unrest (unless it spans several years), one possible approach would be to calculate SO_2 emissions for all volcanic sources based on a 12-month moving average of satellite SO_2 measurements (or shorter for stronger sources). This would conserve the sensitivity of the technique to the weak SO_2 degassing expected in the initial stages of pre-eruptive unrest, whilst permitting more timely identification of increased emissions.

Missing sources and global volcanic CO_2 emissions.　Inevitably, an undetermined number of weaker SO_2 sources, populating the tail of global SO_2 flux distribution (Fig. 4), are missing from the inventory. Continued ground-based SO_2 measurements at low-flux volcanoes[43,55,56] are required to constrain these sources. Such measurements are also needed to improve the relatively poor constraints on the component of global volcanic CO_2 emissions discharged in volcanic plumes[11], which requires *in-situ* determination of the CO_2/SO_2 ratio in the emissions. As shown by Fig. 4, through coordinated efforts such as the Deep Carbon Observatory (DCO; https://deepcarbon.net/)[57] significant progress has been made towards improving the spatial coverage of CO_2/SO_2 measurements, and around 50% of the detected SO_2 sources in Table 1 have characterized CO_2/SO_2 ratios, including many of the strongest sources (Fig. 4), although the frequency of some measurements remains low. Based on our assessment, particular efforts should be made to pursue further CO_2/SO_2 measurements in regions such as Indonesia, Papua New Guinea and Kamchatka, in order to improve constraints on the global volcanic CO_2 flux.

Conclusions

We believe that the volcanic SO_2 emissions inventory described here represents the most accurate assessment of contemporary global volcanic SO_2 degassing, and we encourage its use by the volcanological and atmospheric science communities as a substitute for existing databases[13,31]. Techniques such as this represent a major step forward in monitoring global volcanic degassing and ensure that few, if any, significant sources of volcanic SO_2 will remain undetected in the future, provided that satellite instruments with comparable sensitivity to OMI continue to be deployed (e.g., the Tropospheric Monitoring Instrument [TROPOMI], scheduled for launch on board the Copernicus Sentinel 5-Precursor satellite in 2017; http://www.tropomi.eu). Efforts to further characterize and validate the derived SO_2 emissions are strongly encouraged, particularly at those sources with no prior recorded measurements.

We have highlighted several potential applications of the new inventory, including the identification of regional- and arc-scale trends in SO_2 emissions, and improvement of constraints on global volcanic CO_2 emissions via measurement of CO_2/SO_2 ratios (and their temporal variation) at sources where this information is currently lacking. Ongoing updates to the inventory will potentially provide opportunities to identify pre-eruptive degassing at reawakening volcanoes, and correlate SO_2 flux data with other geophysical data (e.g., ground deformation measured by InSAR) on a larger scale to elucidate volcanic processes. As a final point, the inventory demonstrates the remarkable persistence of passive volcanic degassing, and as anthropogenic SO_2 emissions continue to steadily decline, the volcanic contribution to atmospheric sulfur loading will inexorably increase.

References

1. Oppenheimer, C., Fischer, T. P. & Scaillet, B. Volcanic degassing: process and impact. In: *Treatise on Geochemistry*, 2nd Ed. (eds Holland, H. D. & Turekian, K. K.), Elsevier, Oxford, pp. 111–179, doi: 10.1016/B978-0-08-095975-7.00304-1 (2014).
2. Oppenheimer, C., Scaillet, B. & Martin, R. S. Sulfur degassing from volcanoes: Source conditions, surveillance, plume chemistry and impacts. *Rev. Mineral. Geochem.* **73,** 363–421 (2011).
3. Carn, S. A., Clarisse, L. & Prata, A. J. Multi-decadal satellite measurements of global volcanic degassing. *J. Volcanol. Geotherm. Res.* **311,** 99–134, http://dx.doi.org/10.1016/j.jvolgeores.2016.01.002 (2016).
4. Graf, H.-F., Feichter, J. & Langmann, B. Volcanic sulfur emissions: estimates of source strength and its contribution to the global sulfate distribution. *J. Geophys. Res.* **102,** 10727–10738 (1997).
5. Robock, A. Volcanic eruptions and climate. *Rev. Geophys.* **38,** 191–219 (2000).
6. Hansell, A. & Oppenheimer, C. Health hazards from volcanic gases: A systematic literature review. *Arch. Environ. Health* **59(12),** 628–639 (2004).
7. Longo, B. M., Grunder, A., Chuan, R. & Rossignol, A. SO_2 and fine aerosol dispersion from the Kilauea plume, Kau district, Hawaii, USA. *Geology* **33,** 217–220 (2005).

8. Clarisse, L. *et al.* Retrieval of sulphur dioxide from the infrared atmospheric sounding interferometer (IASI). *Atmos. Meas. Tech.* **5,** 581–594, http://dx.doi.org/10.5194/amt-5-581-2012 (2012).

9. Theys, N. *et al.* Volcanic SO_2 fluxes derived from satellite data: a survey using OMI, GOME-2, IASI and MODIS. *Atmos. Chem. Phys.*, **13,** 5945–5968, doi: 10.5194/acp-13-5945-2013 (2013).

10. Carn, S. A. Multi-Satellite Volcanic Sulfur Dioxide L4 Long-Term Global Database V2, version 2, Greenbelt, MD, USA, Goddard Earth Science Data and Information Services Center (GES DISC), Accessed on Jun 16, 2016, ftp://measures.gsfc.nasa.gov/data/s4pa/SO2/MSVOLSO2L4.2/ (2015).

11. Burton, M. R., Sawyer, G. M. & Granieri, D. Deep carbon emissions from volcanoes. *Rev. Mineral. Geochem.* **75,** 323–354. http://dx.doi.org/10.2138/rmg.2013.75.11 (2013).

12. Pyle, D. M. & Mather, T. A. The importance of volcanic emissions for the global atmospheric mercury cycle. *Atmos. Env.* **37,** 5115–5124 (2003).

13. Andres, R. J. & Kasgnoc, A. D. A time-averaged inventory of subaerial volcanic sulfur emissions. *J. Geophys. Res.* **103,** 25251–25261 (1998).

14. McGonigle, A. J. S. *et al.* Sulphur dioxide fluxes from Papua New Guinea's volcanoes. *Geophys. Res. Lett.* **31,** L08606, http://dx.doi.org/10.1029/2004GL019568 (2004).

15. Hilton, D. R., Fischer, T. P., McGonigle, A. J. S. & de Moor, J. M. Variable SO_2 emission rates for Anatahan volcano, the Commonwealth of the Northern Mariana Islands: Implications for deriving arc-wide volatile fluxes from erupting volcanoes. *Geophys. Res. Lett.* **34,** L14315, doi: 10.1029/2007GL030405 (2007).

16. Bani, P. *et al.* Surge in sulfur and halogen degassing from Ambrym volcano, Vanuatu. *Bull. Volcanol.* **71(10),** 1159–1168 (2009).

17. Galle, B. *et al.* Network for observation of volcanic and atmospheric change (NOVAC)—a global network for volcanic gas monitoring: network layout and instrument description. *J. Geophys. Res.* **115,** D05304, http://dx.doi.org/10.1029/2009JD011823 (2010).

18. Levelt, P. F. *et al.* The Ozone Monitoring Instrument. *IEEE Trans. Geosci. Remote Sens.* **44(5),** 1093–1101, http://dx.doi.org/10.1109/TGRS.2006.872333 (2006).

19. Li, C. *et al.* New-generation NASA Aura Ozone Monitoring Instrument (OMI) volcanic SO_2 dataset: Algorithm description, initial results, and continuation with the Suomi-NPP Ozone Mapping and Profiler Suite (OMPS). *Atmos. Meas. Tech. Discuss.* doi: 10.5194/amt-2016-221, in review (2016).

20. Spinei, E. *et al.* Validation of Ozone Monitoring Instrument SO_2 measurements in the Okmok volcanic cloud over Pullman, WA, July 2008. *J. Geophys. Res.* **115,** D00L08, doi: 10.1029/2009JD013492 (2010).

21. Krueger, A. J. Sighting of El Chichón sulfur dioxide clouds with the Nimbus 7 total ozone mapping spectrometer. *Science* **220,** 1377–1379 (1983).

22. Bluth, G. J. S., Schnetzler, C. C., Krueger, A. J. & Walter, L. S. The contribution of explosive volcanism to global atmospheric sulfur dioxide concentrations. *Nature* **366,** 327–329 (1993).

23. Carn, S. A., Krueger, A. J., Krotkov, N. A., Arellano, S. & Yang, K. Daily monitoring of Ecuadorian volcanic degassing from space. *J. Volcanol. Geotherm. Res.* **176(1),** 141–150 (2008).

24. Campion, R. *et al.* Space- and ground-based measurements of sulfur dioxide emissions from Turrialba volcano (Costa Rica). *Bull. Volcanol.* **74(7),** 1757–1770 (2012).

25. Carn, S. A., Krotkov, N. A., Yang, K. & Krueger, A. J. Measuring global volcanic degassing with the Ozone Monitoring Instrument (OMI). In: Pyle, D. M., Mather, T. A. & Biggs, J. (Eds), Remote Sensing of Volcanoes and Volcanic Processes: Integrating Observation and Modeling. Geol. Soc. Lon, Special Publications 380, http://dx.doi.org/10.1144/SP380.12 (2013).

26. Fioletov, V. E., McLinden, C. A., Krotkov, N., Moran, M. D. & Yang, K. Estimation of SO_2 emissions using OMI retrievals. *Geophys. Res. Lett.* **38,** L21811, doi: 10.1029/2011GL049402 (2011).

27. Fioletov, V. E. *et al.* Application of OMI, SCIAMACHY, and GOME-2 satellite SO_2 retrievals for detection of large emission sources. *J. Geophys. Res.-Atmos.* **118,** 11399–11418, doi: 10.1002/jgrd.50826 (2013).

28. Fioletov, V. E., McLinden, C. A., Krotkov, N. A. & Li, C. Lifetimes and emissions of SO_2 from point sources estimated from OMI. *Geophys. Res. Lett.* **42,** 1–8, doi: 10.1002/2015GL063148 (2015).

29. Fioletov, V. E. *et al.* A global catalogue of large SO_2 sources and emissions derived from the Ozone Monitoring Instrument. *Atmos. Chem. Phys.* **16,** 11497–11519, doi: 10.5194/acp-16-11497-2016 (2016).

30. McLinden, C. A. *et al.* Space-based detection of missing SO_2 sources of global air pollution. *Nat. Geosci.* **9,** 496–500, doi: 10.1038/NGEO2724 (2016).

31. Shinohara, H. Volatile flux from subduction zone volcanoes: Insights from a detailed evaluation of the fluxes from volcanoes in Japan. *J. Volcanol. Geotherm. Res.* **268,** 46–63, doi: 10.1016/j.jvolgeores.2013.10.007 (2013).

32. Li, C., Joiner, J., Krotkov, N. A. & Bhartia, P. K. A fast and sensitive new satellite SO_2 retrieval algorithm based on principal component analysis: application to the ozone monitoring instrument. *Geophys. Res. Lett.* **40,** doi: 10.1002/2013GL058134 (2013).

33. Beirle, S. *et al.* Estimating the volcanic emission rate and atmospheric lifetime of SO_2 from space: a case study for Kilauea volcano, Hawai'i. *Atmos. Chem. Phys.* **14,** 8309–8322, doi: 10.5194/acp-14-8309-2014 (2014).

34. Melnikov, D., Malik, N., Kotenko, T., Inguaggiato, S. & Zelenski, M. A new estimate of gas emissions from Ebeko volcano, Kurile Islands. *Goldschmidt Conference Abstracts*, Yokohama, Japan (2016).

35. Campion, R. New lava lake at Nyamuragira volcano revealed by combined ASTER and OMI SO_2 measurements. *Geophys. Res. Lett.* **41,** 7485–7492, doi: 10.1002/2014GL061808 (2014).

36. Bani, P. *et al.* First arc-scale volcanic SO_2 budget for the Vanuatu archipelago. J. *Volcanol. Geotherm. Res.* **211–212,** 36–46, http://dx.doi.org/10.1016/j.jvolgeores.2011.10.005 (2012).

37. Kern, C. *et al.* Improving the accuracy of SO_2 column densities and emission rates obtained from upward-looking UV-spectroscopic measurements of volcanic plumes by taking realistic radiative transfer into account. *J. Geophys. Res.* **117,** D20302, doi: 10.1029/2012JD017936 (2012).

38. Sutton, A. J. & Elias, T. One hundred volatile years of volcanic gas studies at the Hawaiian Volcano Observatory. In: Characteristics of Hawaiian Volcanoes, *U.S. Geol. Surv. Prof. Pap.* 1801, edited by Poland, M. P., Landowski, C. M. & Takahashi, T. J., pp. 295–320, U.S. Geological Survey, Reston, VA, doi: 10.3133/pp18017 (2014).

39. Schmidt, A. *et al.* Satellite detection, long-range transport, and air quality impacts of volcanic sulfur dioxide from the 2014–2015 flood lava eruption at Bárðarbunga (Iceland). *J. Geophys. Res. Atmos.* **120,** doi: 10.1002/2015JD023638 (2015).

40. Bani, P., Surono, Hendrasto, M., Gunawan, H. & Primulyana, S. Sulfur dioxide emissions from Papandayan and Bromo, two Indonesian volcanoes. *Nat. Hazards Earth Syst. Sci.* **13,** 2399–2407, doi: 10.5194/nhess-13-2399-2013 (2013).

41. Aiuppa, A. *et al.* First determination of magma-derived gas emissions from Bromo volcano, eastern Java (Indonesia). *J. Volcanol. Geotherm. Res.* **304,** 206–213 (2015).

42. Bani, P. *et al.* First measurement of the volcanic gas output from Anak Krakatau, Indonesia. *J. Volcanol. Geotherm. Res.* **302,** 237–241, doi: 10.1016/j.jvolgeores.2015.07.008 (2015).

43. Saing, U. B., Bani, P. & Kristianto. Ibu volcano, a center of spectacular dacite dome growth and long-term continuous eruptive discharges. *J. Volcanol. Geotherm. Res.* **282,** 36–42, doi: 10.1016/j.jvolgeores.2014.06.011 (2014).

44. Smekens, J.-F., Clarke, A. B., Burton, M. R., Harijoko, A. & Wibowo, H. E. SO_2 emissions at Semeru volcano, Indonesia: Characterization and quantification of persistent and periodic explosive activity. *J. Volcanol. Geotherm. Res.* **300,** 121–128, doi: 10.1016/j.jvolgeores.2015.01.006 (2015).

45. Self, S. & King, A. J. Petrology and sulfur and chlorine emissions of the 1963 eruption of Gunung Agung, Bali, Indonesia. *Bull. Volcanol.* **58,** 263–285 (1996).
46. Vidal, C. M. *et al.* The 1257 Samalas eruption (Lombok, Indonesia): the single greatest stratospheric gas release of the Common Era. *Sci. Rep.* **6,** 34868, doi: 10.1038/srep34868 (2016).
47. Self, S. Magma volume, volatile emissions, and stratospheric aerosols from the 1815 eruption of Tambora. *Geophys. Res. Lett.* **31,** 10–13 (2004).
48. Mori, T. *et al.* Time-averaged SO_2 fluxes of subduction-zone volcanoes: Example of a 32-year exhaustive survey for Japanese volcanoes. *J. Geophys. Res. Atmos.* **118,** 8662–8674, doi: 10.1002/jgrd.50591 (2013).
49. Brantley, S. L. & Koepenick, K. W. Measured carbon dioxide emissions from Oldoinyo Lengai and the skewed distribution of passive volcanic fluxes. *Geology* **23,** 933–936 (1995).
50. Sparks, R. S. J., Biggs, J. & Neuberg, J. W. Monitoring volcanoes. *Science* **335,** 1310, doi: 10.1126/science.1219485 (2012).
51. Hickey, Gottsmann, J. J., Nakamichi, H. & Iguchi, M. Thermomechanical controls on magma supply and volcanic deformation: application to Aira caldera, Japan. *Sci. Rep.* **6,** 32691, doi: 10.1038/srep32691 (2016).
52. Jay, J. *et al.* Locating magma reservoirs using InSAR and petrology before and during the 2011–2012 Cordón Caulle silicic eruption. *Earth Planet. Sci. Lett.* **395,** 254–266 (2014).
53. Global Volcanism Program. Report on Asosan (Japan). In: Wunderman, R. (ed.) *Bulletin of the Global Volcanism Network* **40(2),** Smithsonian Institution (2015).
54. Pagli, C. *et al.* Shallow axial magma chamber at the slow-spreading Erta Ale Ridge. *Nat. Geosci.* **5,** 284–287, doi: 10.1038/ngeo1414 (2012).
55. Tamburello, G., Hansteen, T. H., Bredemeyer, S., Aiuppa, A. & Tassi, F. Gas emissions from five volcanoes in northern Chile and implications for the volatiles budget of the Central Volcanic Zone. *Geophys. Res. Lett.* **41,** 4961–4969, doi: 10.1002/2014GL060653 (2014).
56. Stebel, K., Amigo, A., Thomas, H. & Prata, A. J. First estimates of fumarolic SO_2 fluxes from Putana volcano, Chile, using an ultraviolet imaging camera. *J. Volcanol. Geotherm. Res.* **300,** 112–120 (2015).
57. Hazen, R. M. & Schiffries, C. M. Why deep carbon. *Rev. Mineral. Geochem.* **75,** 1–6, http://dx.doi.org/10.2138/rmg.2013.75.1 (2013).
58. Aiuppa, A. *et al.* Total volatile flux from Mount Etna. *Geophys. Res. Lett.* **35,** L24302, doi: 10.1029/2008GL035871 (2008).
59. Grutter, M. *et al.* SO_2 emissions from Popocatépetl volcano: emission rates and plume imaging using optical remote sensing techniques. *Atmos. Chem. Phys.* **8,** 6655–6663, doi: 10.5194/acp-8-6655-2008 (2008).
60. Werner, C. A. *et al.* Degassing of CO_2, SO_2, and H_2S associated with the 2009 eruption of Redoubt Volcano, Alaska, 1989–2006. *J. Volcanol. Geotherm. Res.* **259,** 270–284 (2013).
61. Werner, C. A., Doukas, M. P. & Kelly, P. J. Gas emissions from failed and actual eruptions from Cook Inlet Volcanoes, Alaska, 1989–2006. *Bull. Volcanol.* **73(2),** 155–173 (2011).

Acknowledgements

Author Contributions

S.A.C. analyzed and interpreted the volcanic degassing data, wrote the manuscript and prepared all figures. V.E.F. and C.A.M. developed the algorithm and processed the OMI satellite data. C.L. and N.A.K. provided the OMI satellite data products. All authors reviewed the manuscript.

Additional Information

Supplementary information accompanies this paper at http://www.nature.com/srep

Competing Interests: The authors declare no competing financial interests.

How to cite this article: Carn, S. A. *et al.* A decade of global volcanic SO_2 emissions measured from space. *Sci. Rep.* **7,** 44095; doi: 10.1038/srep44095 (2017).

Publisher's note: Springer Nature remains neutral with regard to jurisdictional claims in published maps and institutional affiliations.